2015 International Nuclear Atlantic Conference - INAC 2015
São Paulo, SP, Brazil, October 4-9, 2015
Associação Brasileira de Energia Nuclear - ABEN
ISBN: 978-85-99141-06-9

BUCKLING MEASUREMENT IN THE IPEN/MB-01 NUCLEAR REACTOR IN CYLINDRICAL CONFIGURATION OF MINOR EXCESS OF REACTIVITY

Rafael Turrini Purgato, Ulysses d´Utra Bitelli, Vitor Ottoni Aredes, Alexandre F. Póvoa da Silva, Diogo Feliciano dos Santos and Ana Cecília de Souza Lima

Instituto de Pesquisas Energéticas e Nucleares (IPEN / CNEN - SP)
Av. Professor Lineu Prestes 2242
05508-000 São Paulo, SP
ubitelli@ipen.br

ABSTRACT

This work presents the results of experimental Buckling in the IPEN/MB-01 nuclear reactor in its cylindrical configuration with 28 fuel rods along its diameter. The IPEN/MB-01 is a zero power reactor designed to operate at a maximum power of 100 watts. It is a versatile nuclear facility, which allows for the simulation of all the characteristics of a nuclear power reactor making it an ideal testbed for this kind of measurement.

A mapping of neutron flux inside the reactor is carried out in order to determine the total Buckling of the cylindrical configuration. The reactor was operated for one hour. Then, the activity of the fuel rods is measured by gamma ray spectrometry using a HPGe solid state detector and a suitable rod scanner. Photon energies of 276.6keV from ^{239}Np (neutron capture (n,?) nuclear reaction) and 293.3keV from ^{143}Ce (fission (n,f) nuclear reaction on both ^{238}U and ^{235}U) , are respectively along both axial and radial directions. Other measurements are performed using gold wires and foils along radial and axial directions of the reactor core.

The three methods above resulted in a weighted average value of 93.18 ± 8.47 m-2 for the Total Buckling of this cylindrical core configuration with 28 control rods along its diameter with 568 fuel rods and only 271 pcm of excess reactivity.

1. INTRODUCTION

IPEN / MB-01 reactor has been used over the years for carrying out numerous experiments in the field of reactor physics. Validation of calculus methodologies and associated nuclear data libraries requires determination of several key parameters when comparing theoretical models to actual experiments [1]. An essential tool for providing such results, IPEN / MB-01 reactor is regarded as benchmark for the NEA Data Bank for critical analysis of experiments [2].

A major advantage of this reactor lies on its operational flexibility. Core geometry can be easily changed by rearranging the layout of fuel rods along a square plate matrix of 30x30 positions. A rectangular (28x26) arrangement using 680 fuel rods is standard for most experiments. Excess reactivity using such configuration is approximately 2500 pcm. Criticality is attained by withdrawing 58.8% of two control rods. Leaving them 41.2% inserted disturbs the distribution of neutron flux, leading to an asymptotic region shorter than the active fuel length (54.8 cm).

An asymptotic region should be free from disturbances caused either by insertion of control rods or proximity to core-reflector (water) boundaries. A cylindrical core using 568 fuel rods (Figure 1) requires only 10% of insertion of control rods to compensate for its small excess reactivity of 271 pcm, leading to less disruption in the flux of neutrons and enlarging its asymptotic extension. The decision of carrying out measurements on a core of lower excess reactivity aims to extend the length of the asymptotic region as much as possible, which is crucial to obtain more accurate values of Buckling parameter which is merely a measurement of the bending of neutrons flow within the reactor core, allowing for more precise parameters that can later serve as a standard for comparison with values obtained from calculations using reactor physics computer programs. As we shall see, the Buckling is a parameter related to the likelihood of neutrons escaping from the reactor core. The cylindrical shape of the core benefits from reduced neutron escape when compared to both rectangular and square core geometries, substantially contributing to nuclear fuel saving. In the asymptotic region, the neutron flux behaves as a cosine function along the axial direction, whereas in the radial direction it follows a Bessel function instead.

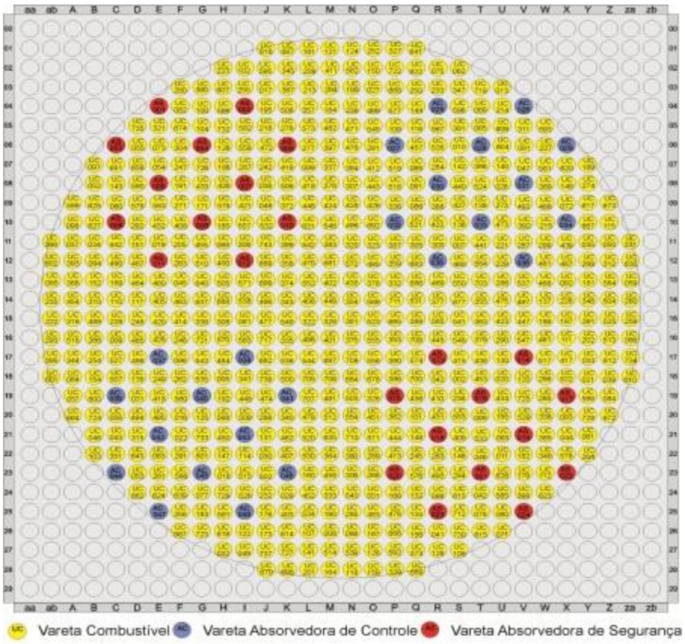

Figure 1: Cylindrical reactor configuration with Lesser Excess of Reactivity

Experimentally the neutron flux can be determined by gamma-ray spectrometry of fuel rods on gold wire irradiated. This technique based on low background High Purity Germanium (HPGe) detectors is applied after irradiation of the samples [1]. Several samples can be irradiated simultaneously at different positions inside the reactor core. The values obtained allow knowing the curvature of the neutron flux (Buckling) [2].

The geometric buckling of cylindrical reactors can be determined by equation 1 [3]:

$$B_g^2 = \left(\frac{2{,}405}{R_{eff}}\right)^2 + \left(\frac{\pi}{H_{eff}}\right)^2 \qquad (1)$$

where:

B_g is the geometric Buckling;
R_{eff} is the effective radius obtained in the radial direction.
He_{ff} is the effective height with measurements obtained in the axial direction.

The values of effective radius and height are obtained experimentally from detection range and computational calculations.

So if we measure by extrapolating the distance to which the neutrons flux bends down to be canceled along the radial direction (Reff) and along the axial direction (Heff) of the reactor core fuel rods, next to the central orthogonal axes and introducing the experimental results, it is possible to obtain the Buckling for this reactor core geometric configuration.

2. METHODOLOGY

For the experimental data acquisition it was used the technique of irradiating fuel rods, gold wire and gold foil. For the fuel rods, the reactor was operated at 30 watts for one hour. A new fuel rod was used to acquire data in order to map the axial neutron flux, located in the central region of the reactor core.

The activity of the fuel rods irradiated was measured using a Hyper Pure Germanium solid state detector (HPGe). Epithermal neutron flux profile was obtained through the analyses of ^{239}Np of 276.6keV photon energy with 14.28% probability of emission.

To measure the relative profile of thermal neutron flux was analyzed the ^{143}Ce photon energy of 293.3keV with 42.8% probability of emission. ^{143}Ce is a product of ^{235}U fission by thermal neutrons and has the advantages of having a reasonable fission yield (~ 6%) and a sufficiently long half-life (33 hours) for a spectral analysis of gamma rays.

The radial flow was measured for the directions north-south and east-west. The count (C_{net}) obtained with the detector was held at 364mm axial dimension (Figure 2) which corresponds to half the active length of the core. The Real Time considered was 1800 seconds.

Axial Counts (C_{net}) were obtained considering the gamma photopic from ^{239}Np and ^{143}Ce emission energies in 29 different axial regions separated 20mm from each other, lasting 30 minutes for each region. The fuel rod used for the measurement was taken from the central position of the reactor core.

The counts were corrected due to decay, equation 2, and deviations in the rates of corrected counts were considered, equation 3, using the decay constants of ^{239}Np ($\lambda = 3.41 \text{ x}10^{-6} \text{ s}^{-1}$) and ^{143}Ce ($\lambda = 5.83\text{x}10^{-6} \text{ s}^{-1}$).

$$C_{cor} = \frac{C_{Net}}{LT} \, e^{\lambda TE} \qquad (2)$$

$$\sigma^2_{C_{cor}} = \left(\frac{C_{cor}}{C_{Net}}\right)^2 \sigma^2_{C_{Net}} \qquad (3)$$

In order to obtain the corrected counts, was essential to record the waiting time between the end of each irradiation and its respective time of measurement (TE).

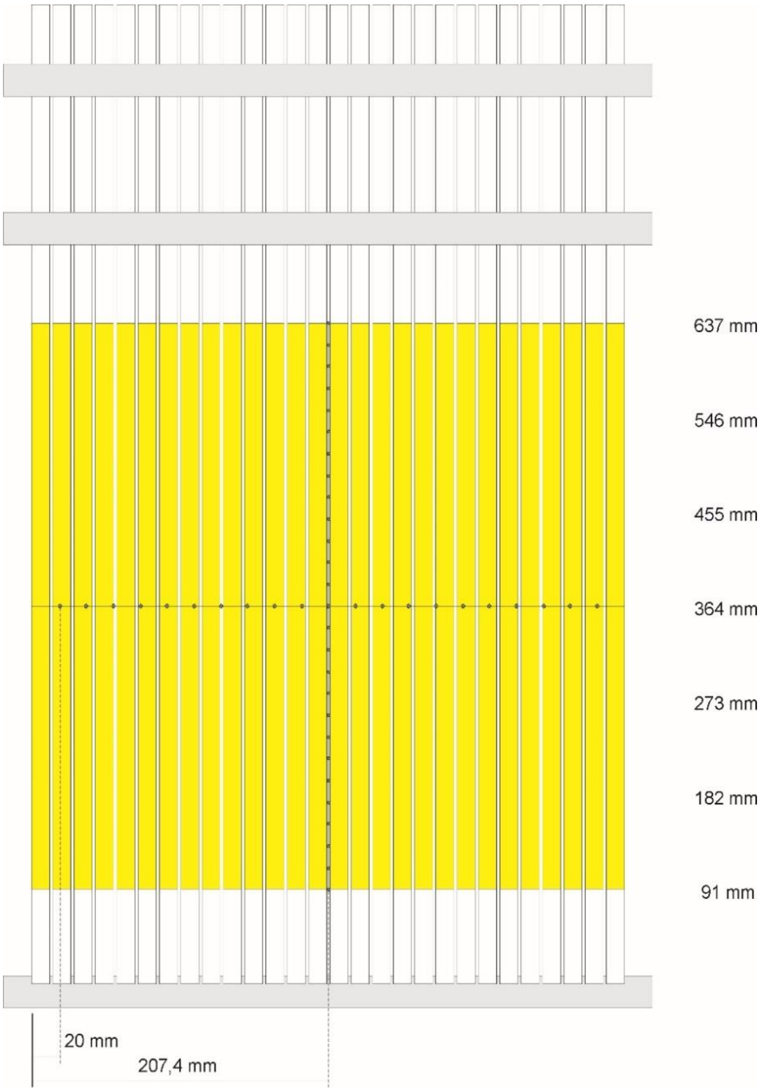

Figure 2: Lateral view of IPEN/MB-01 reactor showing activation positions (black spots).

Similarly, two irradiations were performed for the gold wires, one for the axial direction and another for the radial direction, both at central location in the reactor core. The irradiation was carried out at full power operation of the reactor IPEN/MB-01, that is, 100watts. The irradiation times were two hours for the axial direction and one hour for the radial direction. The same conditions and equations, (2) and (3), used for the fuel rods, were used for the gold wires. However, scores were recorded every 20 mm along the wire and the duration was one hour for each position above mentioned. It was considered that the decay constant for gold is λ = 2.97 x10-6 s^{-1}.

The gold wires were placed on an acrylic plate in order to irradiate and precisely positioning them in the center of the reactor core. The system was irradiated during one hour by 100 watts.

After the data acquisition, Origin software was applied to calculate the effective radius and height for both radial and axial directions. Cosine function was applied for axial data and Bessel function was used for radial data analysis.

2015 International Nuclear Atlantic Conference - INAC 2015
São Paulo, SP, Brazil, October 4-9, 2015
Associação Brasileira de Energia Nuclear - ABEN
ISBN: 978-85-99141-06-9

3. RESULTS

Corrected counts values as a function of fuel rods position are shown in this section. Detailed results are available in reference 5.

Figure 3 shows the distribution profile of ^{239}Np epithermal neutron flux along East-West radial direction as well as the polynomial fit used to determine its effective radius.

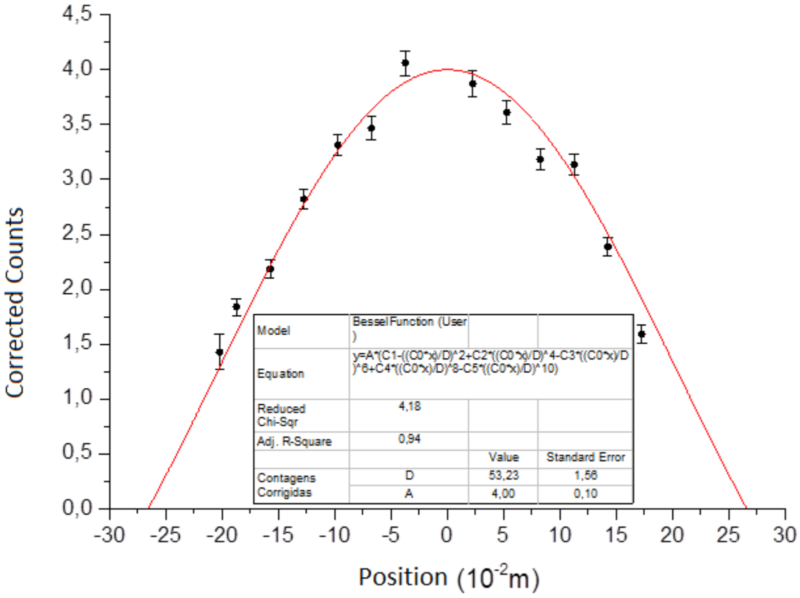

Model	BesselFunction (User)		
Equation	y=A*(C1-((C0*x)/D)^2+C2*((C0*x)/D)^4-C3*((C0*x)/D)^6+C4*((C0*x)/D)^8-C5*((C0*x)/D)^10)		
Reduced Chi-Sqr	4,18		
Adj. R-Square	0,94		
		Value	Standard Error
Contagens Corrigidas	D	53,23	1,56
	A	4,00	0,10

Figure 3: ^{239}Np normalized Count Rates along East-West direction.

Figure 4 shows the distribution profile of ^{143}Ce thermal neutron flux along East-West radial direction as well as the polynomial fit used to determine its effective radius.

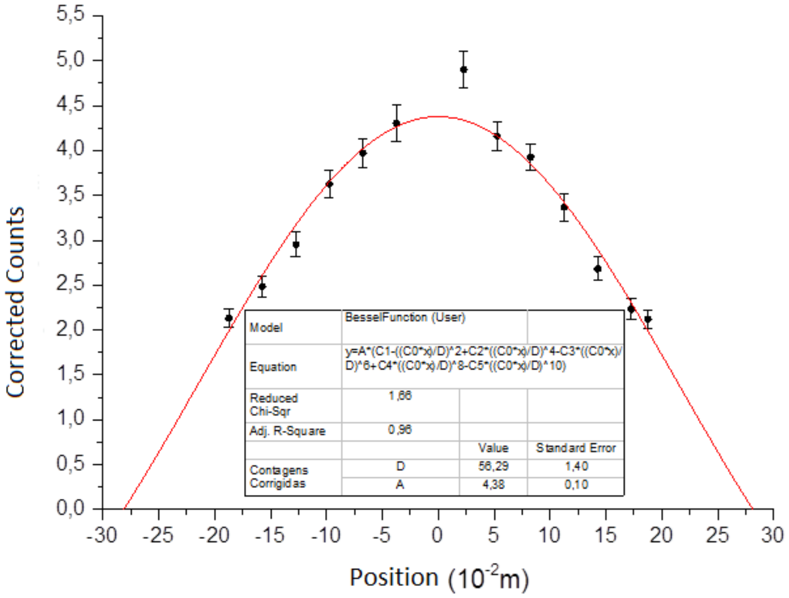

Model	BesselFunction (User)		
Equation	y=A*(C1-((C0*x)/D)^2+C2*((C0*x)/D)^4-C3*((C0*x)/D)^6+C4*((C0*x)/D)^8-C5*((C0*x)/D)^10)		
Reduced Chi-Sqr	1,66		
Adj. R-Square	0,96		
		Value	Standard Error
Contagens Corrigidas	D	56,29	1,40
	A	4,38	0,10

Figure 4: ^{143}Ce normalized Count Rates along East-West direction.

Figure 5 shows the distribution profile of ^{239}Np epithermal neutron flux along North-South radial direction as well as the polynomial fit used to determine its effective radius.

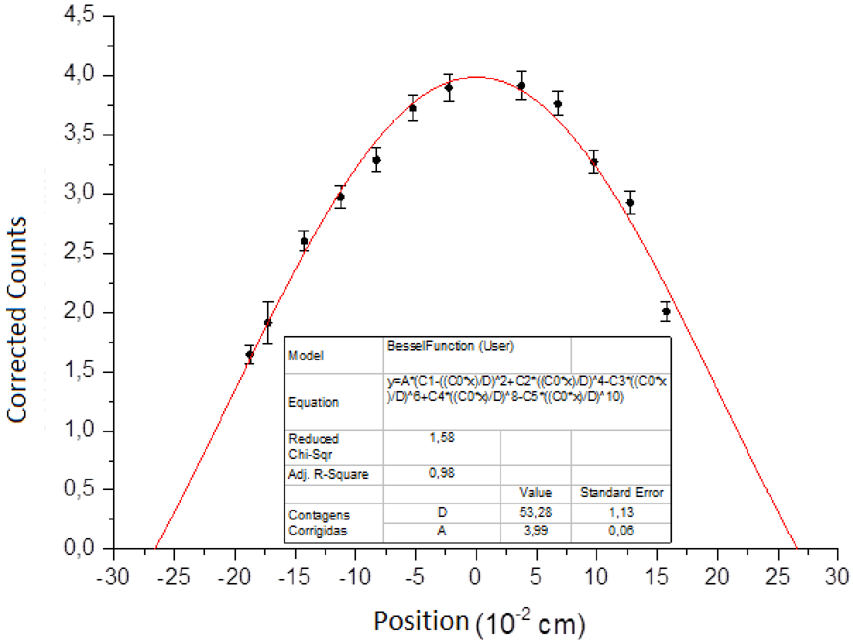

Model	BesselFunction (User)		
Equation	y=A*(C1-((C0*x)/D)^2+C2*((C0*x)/D)^4-C3*((C0*x)/D)^6+C4*((C0*x)/D)^8-C5*((C0*x)/D)^10)		
Reduced Chi-Sqr	1,58		
Adj. R-Square	0,98		
		Value	Standard Error
Contagens Corrigidas	D	53,28	1,13
	A	3,99	0,06

Figure 5: ^{239}Np normalized Count Rates along North-South direction.

Figure 6 shows the distribution profile of ^{143}Ce thermal neutron flux along North-South radial direction as well as the polynomial fit used to determine its effective radius.

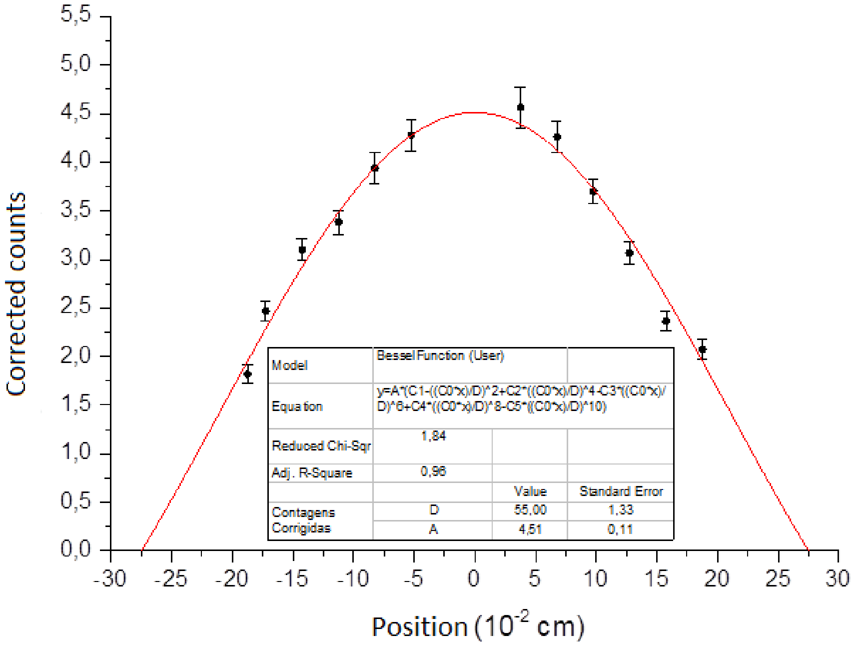

Model	Bessel Function (User)		
Equation	y=A*(C1-((C0*x)/D)^2+C2*((C0*x)/D)^4-C3*((C0*x)/D)^6+C4*((C0*x)/D)^8-C5*((C0*x)/D)^10)		
Reduced Chi-Sqr	1,84		
Adj. R-Square	0,96		
		Value	Standard Error
Contagens Corrigidas	D	55,00	1,33
	A	4,51	0,11

Figure 6: ^{143}Ce normalized Count Rates along North-South direction.

Figures 7 and 8 show measurements derived from the rod at the center of the core along its axial direction and the polynomial fits used to determine their effective radius.

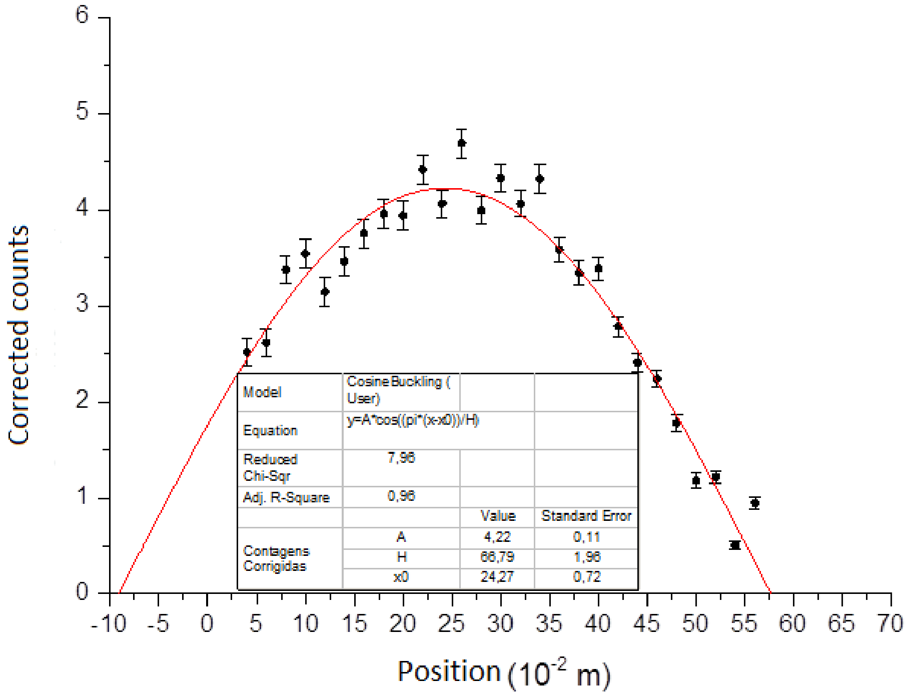

Model	Cosine Buckling (User)		
Equation	y=A*cos((pi*(x-x0))/H)		
Reduced Chi-Sqr	7,96		
Adj. R-Square	0,96		
		Value	Standard Error
Contagens Corrigidas	A	4,22	0,11
	H	66,79	1,96
	x0	24,27	0,72

Figure 7: ^{239}**Np curve fitted along axial direction for epithermal neutrons count.**

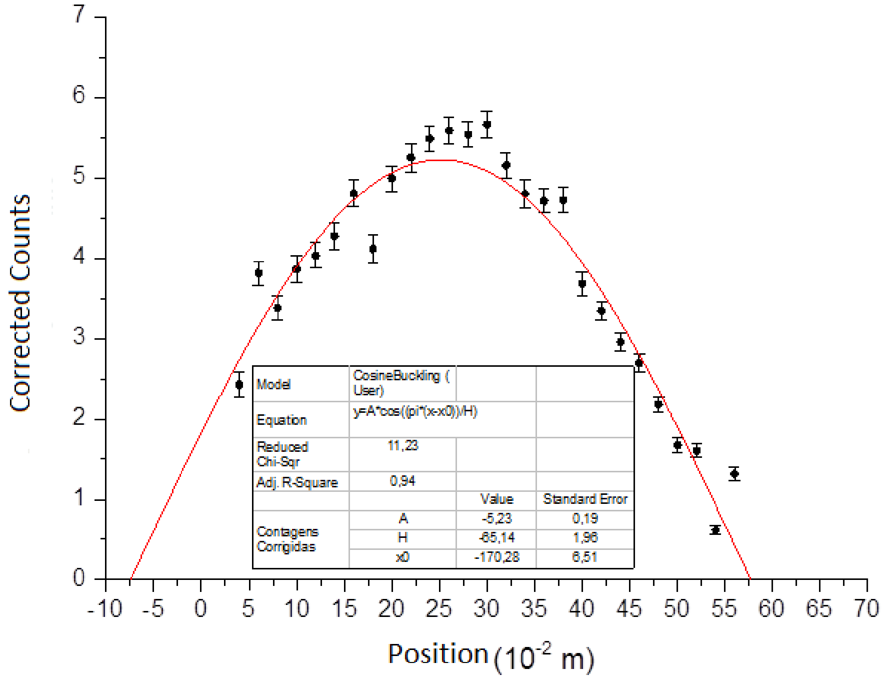

Model	CosineBuckling (User)		
Equation	y=A*cos((pi*(x-x0))/H)		
Reduced Chi-Sqr	11,23		
Adj. R-Square	0,94		
		Value	Standard Error
Contagens Corrigidas	A	-5,23	0,19
	H	-65,14	1,96
	x0	-170,28	6,51

Figure 8: ^{143}**Ce curve fitted along axial direction for thermal neutrons count.**

Effective radius and height could be obtained from curve fit parameters according to Figures 2 through 7, as well as the total Buckling for both thermal and epithermal neutrons.

Neutron flux profiles derived from gold wires scanning along both radial and axial positions are shown in Figures 9 and 10.

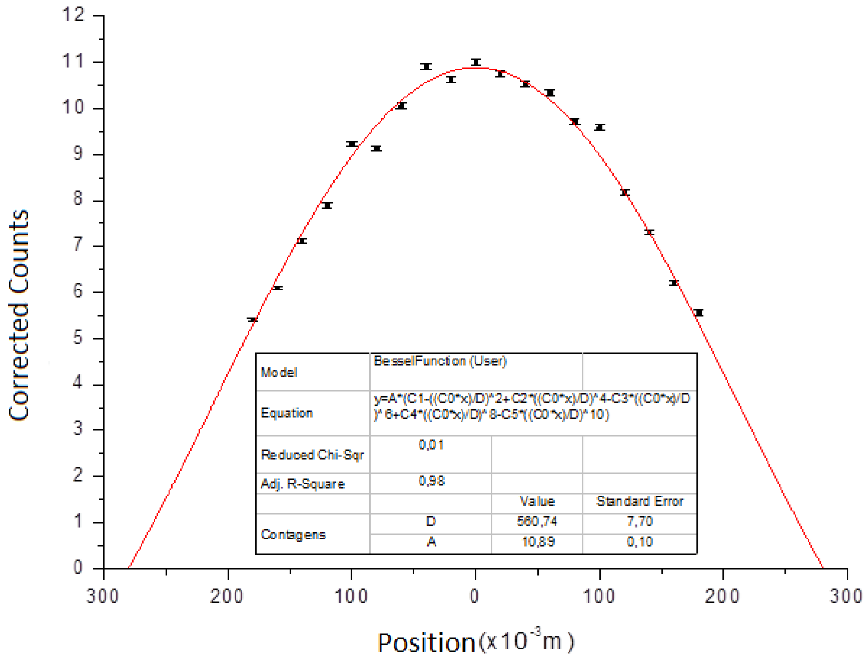

Model	BesselFunction (User)		
Equation	y=A*(C1-((C0*x)/D)^2+C2*((C0*x)/D)^4-C3*((C0*x)/D)^6+C4*((C0*x)/D)^8-C5*((C0*x)/D)^10)		
Reduced Chi-Sqr	0,01		
Adj. R-Square	0,98		
		Value	Standard Error
Contagens	D	560,74	7,70
	A	10,89	0,10

Figure 9: curve fitted along radial direction using gold wire for both thermal and epithermal neutrons count.

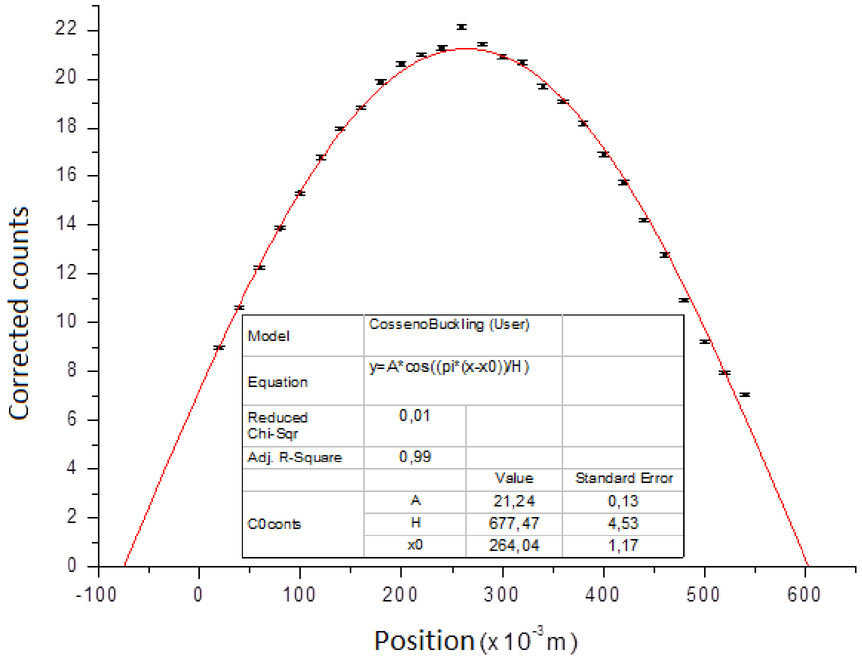

Model	CossenoBuckling (User)		
Equation	y=A*cos((pi*(x-x0))/H)		
Reduced Chi-Sqr	0,01		
Adj. R-Square	0,99		
		Value	Standard Error
C0conts	A	21,24	0,13
	H	677,47	4,53
	x0	264,04	1,17

Figure 10: curve fitted along axial direction using gold wire for both thermal and epithermal neutrons count.

Effective radius and height of the reactor core as well the full Buckling (1) for the cylindrical configuration can be derived from gold wire measurements.

Neutron flux profiles obtained from gold foils along both radial and axial directions are shown in Figures 11 and 12, respectively.

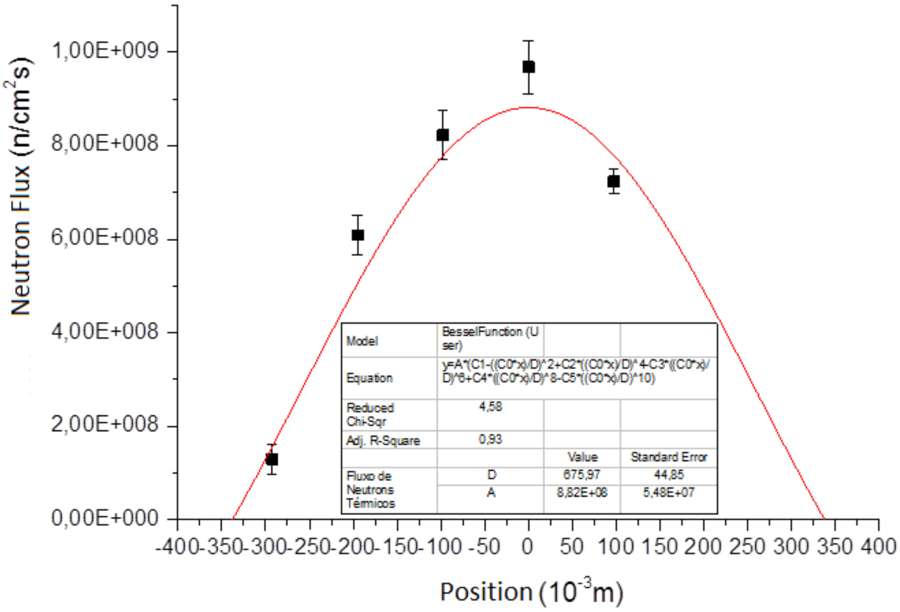

Model	BesselFunction (User)		
Equation	y=A*(C1-((C0*x)/D)^2+C2*((C0*x)/D)^4-C3*((C0*x)/D)^6+C4*((C0*x)/D)^8-C5*((C0*x)/D)^10)		
Reduced Chi-Sqr	4,58		
Adj. R-Square	0,93		
		Value	Standard Error
Fluxo de Neutrons Térmicos	D	675,97	44,85
	A	8,82E+08	5,48E+07

Figure 11: curve fitted along radial direction using gold foils for thermal neutrons count.

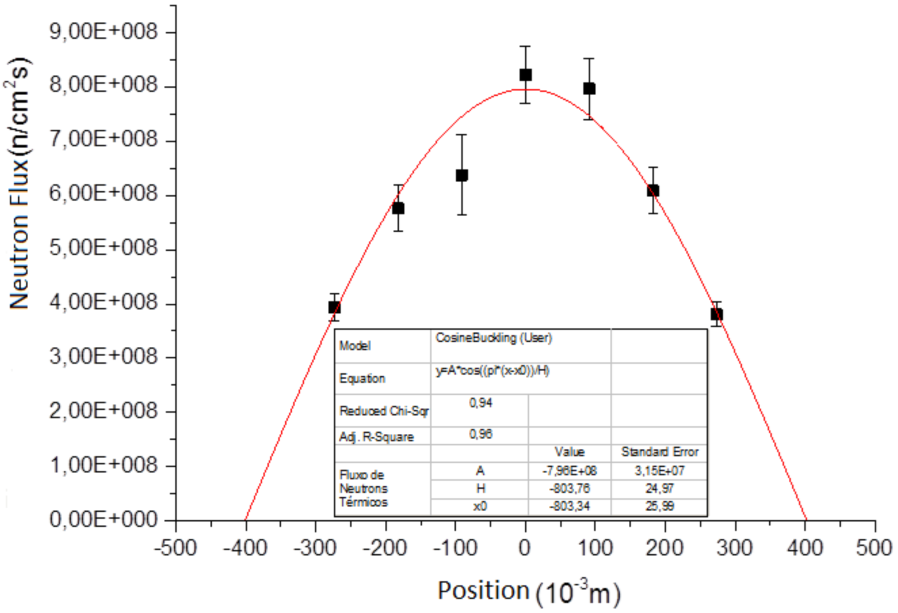

Model	CosineBuckling (User)		
Equation	y=A*cos((pi*(x-x0))/H)		
Reduced Chi-Sqr	0,94		
Adj. R-Square	0,96		
		Value	Standard Error
Fluxo de Neutrons Térmicos	A	-7,96E+08	3,15E+07
	H	-803,76	24,97
	x0	-803,34	25,99

Figure 12: curve fitted along axial direction using gold foils for thermal neutrons count.

Effective radius and height of IPEN/MB-01 reactor core as well as its full Buckling for this configuration can be derived from gold foils measurements.

Based on the data obtained from the four calculations performed for the measurement of buckling, total buckling reactor is determined from the weighted average of those four measurements, including propagation of their associated uncertainties [4].

Table 1 summarizes overall results from each measurement realized throughout this work.

Table 1: *Buckling* (B^2) measurement results from IPEN/MB-01 nuclear reactor.

Method	B^2 (m^{-2})
^{239}Np (Thermal + Epithermal)	103.37 ± 3.57
^{143}Ce, (Thermal + Epithermal)	99.45 ± 3.84
G. Wire 1 (Thermal + Epithermal)	95.09 ± 2.04
G. Wire 2 (Thermal + Epithermal)	84.06 ± 3.01
Gold Wire 1 (Thermal)	97.33 ± 2.34
Gold Wire 2 (Thermal)	84.51 ± 3.48
Gold Wire 1 (Epithermal)	97.20 ± 1.21
Gold Wire 2 (Epithermal)	86.70 ± 3.29
Total	**93.18 ± 8.47**

Based on the Buckling results from fuel rods and gold wires, it was possible to obtain the non-leakage probability. The calculation was realized in order to obtain the thermal non-leakage probability (P_T), the fast non-leakage probability (P_F) and the fast and thermal non-leakage probability (P_{TF}).

Theory shows that the probability of non-escape of thermal neutrons (PT) and non-escape fast neutrons (PF) are given by equations (4) and (5) [3,5], where B2 is the measured Buckling reactor, L2 is the diffusion area of thermal neutrons, and τ is the age of Fermi which corresponds to 1/6 of the shortest travel path squared, from the point where fast neutrons originate to the point where they are heavily moderated, while the diffusion area corresponds to 1/6 of the shortest neutrons path squared, from the point where they become thermal to the point where they vanish from the system by either absorption or escape.

Using a model for two neutron energy ranges, the total probability of neutron leakage from the system (PTF) is given by equation (6):

$$P_T = \frac{1}{1+B^2.L^2} \tag{4}$$

$$P_F = \frac{1}{1+B^2.\tau} \tag{5}$$

$$P_{TF} = P_T.P_F \tag{6}$$

Applying four neutron energy ranges to Hammer-Technion code [6], L^2 and τ parameters for IPEN / MB-01 reactor were estimated in 30.59 cm^2 and 1.91 cm^2 [2.5], respectively.

Buckling values were measured using different techniques. Results and their weighted average are summarized in Table 2.

Admitting a fast and thermal non-leakage probability (PTF) of 76.47±1.66%, nuclear reactor leakage can be estimated around 24%.

Table 2: Thermal non-leakage probability (P_T), Fast non-leakage probability (P_F), and Thermal + Fast non-leakage probability (P_{TF}) for both fuel rods and gold wires.

	P_T (%)	P_F (%)	P_{TF} (%)
^{239}Np Integral Counts	75.98 ± 2.63	98.07 ± 3.46	**74.51 ± 3.68**
^{143}Ce Integral Counts	76.68 ± 2.96	98.14 ± 3.87	**75.25 ± 4.15**
G. Wire 1 Integral Counts	77.47 ± 1.66	98.22 ± 2.15	**76.09 ± 2.33**
G. Wire 2 Integral Counts	79.55 ± 2.85	98.42 ± 3.58	**78.29 ± 4.00**
G. Wire 1 Separated Counts	77.06 ± 1.85	98.18 ± 1.24	**75.66 ± 2.05**
G. Wire 2 Separated Counts	79.46 ± 3.28	98.37 ± 3.79	**78.17 ± 4.41**
Weighted Average	**77.83 ± 1.60**	**98.24 ± 0.22**	**76.47 ± 1.66**

4. CONCLUSIONS

Results from the present work let state that the Buckling of the reactor can be foreseen as a measure of neutrons escaping from it; the smaller the size of the core, the larger the buckling, with steeper curvatures of neutron flux eventually yielding to higher neutron leakage.

Steeper curvatures were noticed for epithermal neutrons in the case of rods as indicated by the larger associated values of Buckling. Such result was already expected due to their higher energy when compared to thermal neutrons.

Higher Buckling values were observed along radial direction. This was expected because of the smaller reactor core dimension along that direction, also leading to higher leakage flux.

It could also be checked that the Buckling is independent of operation power. As its level rises, neutron flux rises proportionally along every dimension, preserving the shape of neutron flux distribution.

The weighted average of all four results led to a Total Buckling of **93.18 ± 8.47 m^{-2}** for the cylindrical configuration used during this work on IPEN/MB-01 reactor.

ACKNOWLEDGMENTS

Our acknowledgments to all the staff of the IPEN/MB-01 reactor of The Centre for Nuclear Engineering (CEN) of Institute of Nuclear and Energy Research, for their support, assistance and knowledge sharing during the experiments, specially to Mr. Rogério Jerez, Hugo Rodrigues Landim e Cesar Luiz Veneziani.

REFERENCES

1. Bitelli, U.U ; Santos, A. dos; Jerez, R.; Diniz, R.; Fanaro, L. C. C. B.; Abe, A. Y.; Moreira, J. M. L.; Fér, N.; Giada, M. R.; Fuga, R.. Experimental Utilization of the IPEN/MB-01 Reactor. In: 9th Meeting of the International Group on Research Reactor, 2003, Sydney, 2003.
2. S*antos, A.et al .Leu-comp-therm-077 Critical loading configuration of the ipem/mb-01 reactor. Blair Briggs, J (Ed.) International Handbook of Evaluated Critixality Safety Benchmark Experiments, 2004 . September ed. Nuclear Energy Agency, Paris, NEA/NSC/DOC (95) 03/1.*
3. Lamarsh - *Theory of Nuclear Reactors*, New York University, EUA.
4. Zijp, W. L*., Treatment of Measurement Uncertainties*, ECN-194, January (1987).
5. Purgato, R. T., Medida do Buckling e da Probabilidade de Fuga de Nêutrons do Núcleo do Reator IPEN/MB-01, Dissertação de Mestrado, São Paulo (2014).
6. Suich,J.E;Honeck,H.C. The Hammer System Heterogeneous Analysis of Multigroup Methods of Exponential and Reactor. Aiken, S.C., Du Pont de Nemours Riber Laboratory (DP-1064), 1967.